

state is more effective than the transient state. For the brief equivalent circuits, a model of induction motors can be remodeled such as Fig. 2. Here, R_{qls} , R_{dls} , R_{qlr} , and R_{dlr} are the stator and rotor resistances of the iron loss. The remodeled equivalent circuits can be obtained by the following assumptions.

- 1) The model is based on the steady state in the field-oriented frame.
- 2) The leakage flux is too small in comparison with the flux to be considered.
- 3) All parameters of the induction motor are regarded as constants because all parameters are not taken into account of the flux saturation and the temperature.
- 4) The rotor resistance of the iron loss is regarded as part of the rotor resistance. ($R_r = R_r \parallel R_{qlr}$)

With the above assumption, the following equations are acquired from the equivalent circuits in the steady state.

$$\lambda_{qr}^e = 0 = \lambda_{qs}^e = M_q (i_{qms}^e + i_{qmr}^e) \quad (1)$$

$$i_{qms}^e = -i_{qmr}^e \quad (2)$$

$$v_{dls}^e = 0 = v_{dlr}^e \quad (3)$$

$$i_{dms}^e = i_{ds}^e \quad (4)$$

$$i_{dls}^e = 0 = i_{dlr}^e \quad (5)$$

$$\lambda_{ds}^e = \lambda_{dr}^e = M_d (i_{dms}^e + i_{dlr}^e) \quad (6)$$

$$\lambda_{ds}^e = \lambda_{dr}^e = M_d i_{ds}^e \quad (7)$$

From the equation in (4), the iron loss of the d-axis is zero; R_{dls} in Fig. 2 is also zero. Therefore, the total iron loss is equal only to the one of the q-axis. The circuits of the q-axis in Fig. 2 is formulated as the following.

$$(\omega_e - \omega_r) M_d i_{ds}^e = R_r i_{qms}^e \quad (8)$$

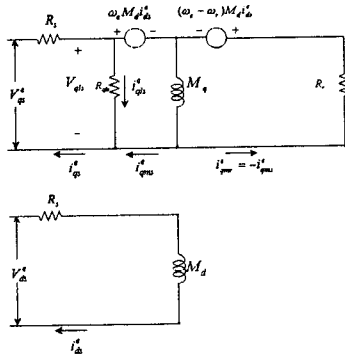


Fig. 2. Brief equivalent circuits of IM at the steady state in field-oriented frame

From the equation (8) and Fig. 2,

$$i_{qms}^e = i_{qs}^e - \frac{v_{qls}}{R_{qls}} = i_{qs}^e - \left(\frac{R_r}{M_d} \frac{i_{qms}^e}{i_{ds}^e} + \omega_r \right) \left(\frac{M_d}{R_{qls}} i_{ds}^e \right) \quad (9)$$

In sum,

$$i_{qms}^e = \left(\frac{R_{qls}}{R_{qls} + R_r} \right) i_{qs}^e - \left(\frac{M_d}{R_{qls} + R_r} \right) \omega_r i_{ds}^e \quad (10)$$

Based on the above equations, the iron and copper losses of the induction motor are illustrated as

$$P_{cus} = R_s \left((i_{ds}^e)^2 + (i_{qs}^e)^2 \right) \quad (11)$$

$$P_{cur} = R_r (i_{qmr}^e)^2 \quad (12)$$

$$P_{fe} = R_{qls} (i_{qs}^e - i_{qms}^e)^2 \quad (13)$$

$$P_t = P_{cus} + P_{fe} + P_{cur} \quad (14)$$

$$= R_q (i_{qs}^e)^2 + R_d \omega_r (i_{ds}^e)^2$$

where,

$$R_q \equiv R_s + \frac{R_{qls} R_r}{R_{qls} + R_r}$$

$$R_d \equiv R_s + \frac{M_d^2}{R_{qls} + R_r} \omega_r^2$$

P_{cus} : stator copper loss

P_{cur} : rotor copper loss

P_{fe} : iron loss

P_t : total loss.

The torque of the induction motor are represented by following equations.

$$T_d = p (\lambda_{qr}^e i_{dmr}^e - \lambda_{dr}^e i_{qmr}^e) \quad (15)$$

$$T_d = p \left(\frac{M_d i_{ds}^e}{R_{qls} + R_r} (R_{qls} i_{qs}^e - M_d \omega_r i_{ds}^e) \right) \quad (16)$$

$$T_d \cong p M_d i_{ds}^e i_{qs}^e \quad (17)$$

where,

$$R_{qls} \gg R_r$$

$$R_{qls} \gg (M_d)^2 \omega_r (i_{ds}^e)^2$$

3. Optimal efficiency control algorithm

We are able to achieve the optimal ratio ($K_{\min(\omega)}$) which minimizes the loss in the model. The derivative for the time in (14) is

$$i_{ds}^e = K_{\min(\omega)} | i_{qs}^e | \quad (18)$$

where,

$$K_{\min(\omega)} = \sqrt{\frac{R_q}{R_d}} = \sqrt{\frac{R_s (R_{qls} + R_r) + R_{qls} R_r}{R_s (R_{qls} + R_r) + M_d^2 \omega_r^2}} \quad (19)$$

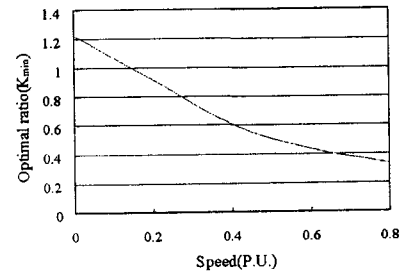


Fig.3 Relations between loss-minimization factor and speed

Figure 3 shows relations between the loss-minimization factor and the speed. It is impossible to apply the optimal efficiency algorithm in case of the low speed region because an optimal ratio exceeds 1.

From (14)-(17), the efficiency of the induction motor can be obtained as follows

$$\eta = \frac{T_d \omega_r}{T_d \omega_r + P_i} \quad (20)$$

where,

$$T_d \omega_r = M_d i_{qs}^e i_{ds}^e \omega_r$$

$$P_i = \left(R_s + \frac{R_{qls} R_r}{R_{qls} + R_r} \right) (i_{qs}^e)^2 + \left(R_s + \frac{M_d^2 \omega_r^2}{R_{qls} + R_r} \right) (i_{ds}^e)^2$$

As the rotor flux becomes smaller, the flux current is reduced, but the torque increases through the speed controller. Consequently, the torque of the motor remains constant. The reduction of the flux brings in the increase of the copper loss and the reduction of the iron loss. It results in the reduction of the DC link input power.

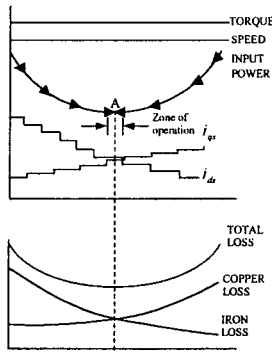


Fig. 4 Principle of efficiency optimization control

This paper proposes the equation to obtain the minimal of the input power. At the steady state, the minimum point of input power can be obtained as shown in Fig. 4. Based on the Fig. 4, the value of total loss is the lowest when the copper corresponds iron loss. On the supposition that the torque is constant in the steady state, when the flux and torque currents optionally control the torque, the value of the point from (17)-(20) can be calculated by (21)

$$\hat{T}_d = K_t i_{ds}^* i_{qs}^* = K_t i_{ds}^{e*} i_{qs}^{e*} \quad (21)$$

where,

\hat{T}_d : constant torque in the steady state

i_{ds}^{e*} : flux current in the steady state

i_{qs}^{e*} : torque current in the steady state

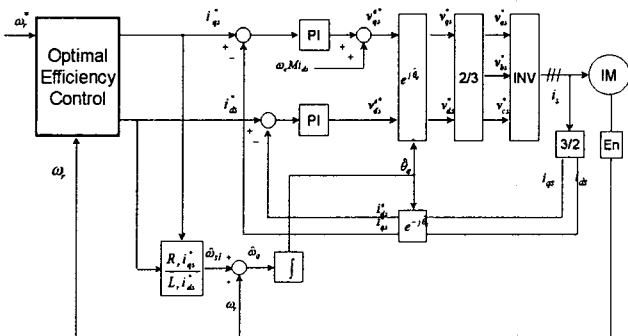


Fig. 5 Block diagram of the proposed system

As a consequence, we can get the lowest value of loss with the flux and torque currents derived from the optimal ratio. Along with this, the optimal efficiency control is

established. However, this algorithm has a disadvantage. The transient state, characterized as the load torque variations, requires a lot of time. It is caused by the fact that the only flux current, acquired by the proposed control method, fails to get the plenty of torque within the short time. Therefore, to solve this problem, the enough torque can be facilitated by the nominal flux current in the transient state. This system can be used only under the steady state, defined as the state in which the speed error is within 0.5%. Therefore, the nominal flux current should be applied in the transient state. The block diagram for the optimal efficiency control of the induction motor is shown in Fig.5. Figure 6 shows the block diagram of the proposed controller. As Fig. 6, the optimal method should be adapted if the real speed is within 0.5% of the reference speed. Otherwise, the constant flux current should be permitted in the system.

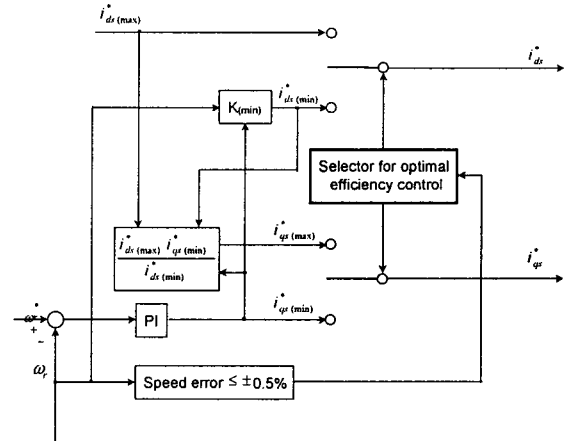


Fig.6. Block diagram of the optimal efficiency controller

4. Computer simulations and experimental results

The overall block diagram for the induction motor drives is shown in Fig.7. The actual parameters of an induction motor used for the experiments are listed in the appendix. The rotor shaft of the induction motor is connected to the loaded DC generator. A 3.3(KW) DC generator has been applied for the loads. The hardware of the experimental system has been implemented by a 32 bit floating point TMS320C32 DSP. The calculations except for the motion controller(ADMC201 IC) are performed by DSP with the sampling time of 100 [μsec]. The space vector PWM controller is performed by about 10[KHz] switching frequency of the IGBT inverter. The motor speed is measured by an optical encoder installed at the motor shaft. The encoder pulses which generate 6000 pulses per revolution are increased to 24000 pulses per revolution by using a multiply-by-four logic circuit.

Because the proposed controller is only operated in the steady state, the steady state is considered to be within 0.5% of the reference speed. When the real speed reaches to the considered steady state, the optimal reference of the torque and flux currents does not control the system just at the moment. To avoid an unstable drive condition of induction motors given rise to sudden reference variations, optimal values divide into 20 steps per 0.06 second from the reference currents of the transient state to the reference

currents of the steady state. From the process, we can get the maximum efficiency point within 1.2 second.

To verify the capacities of the proposed control schemes, speed references of 1500rpm are enforced at 0.1 times rating load. Figure 8 shows the rotor speed, the reference of flux current, the torque current, torque, and input power by the computer simulations. Under the same torque condition, we can show the waveforms of the minimum input power.

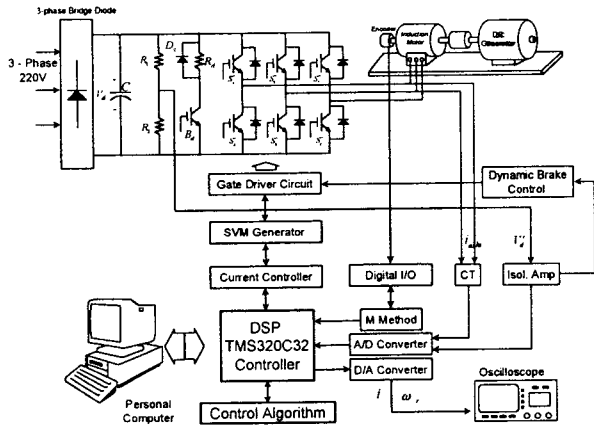
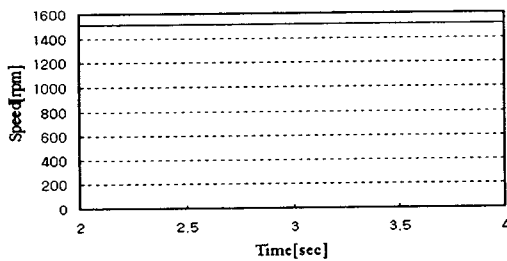
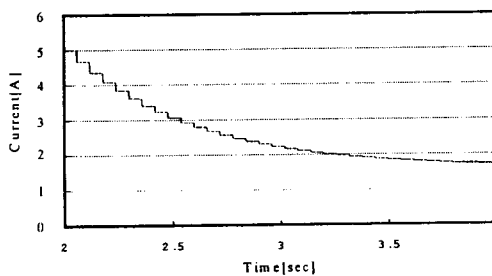


Fig. 7 Hardware block diagrams of IM

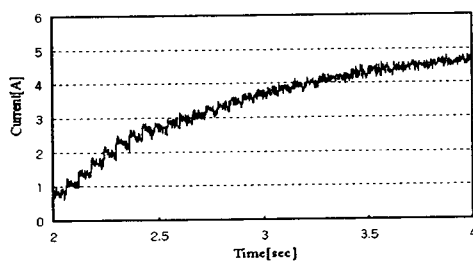
To verify the motor performance by the proposed control schemes in the transient state, the reference of rotor speed gives from 500 to 1000[rpm]. In Fig. 9, even the torque and speed are varied, we can see the good performance.



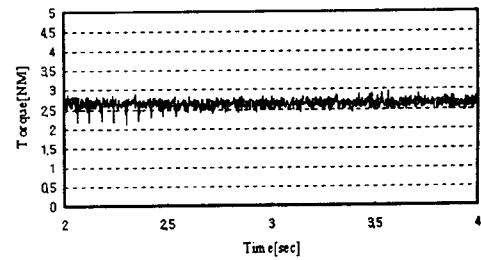
(a) rotor speed



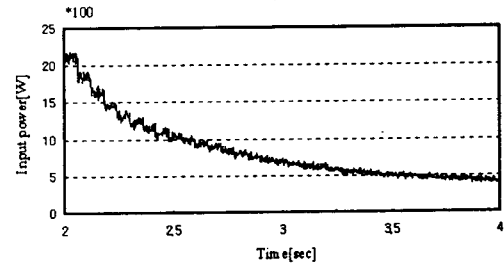
(b) reference of flux current



(c) torque current

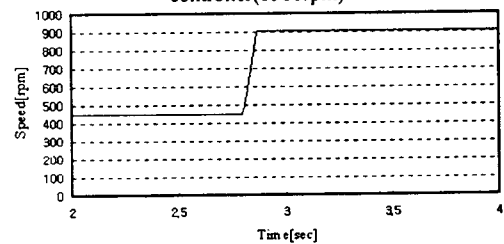


(d) torque

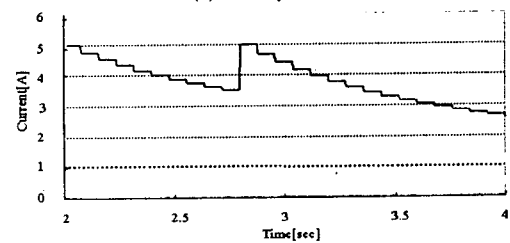


(e) input power

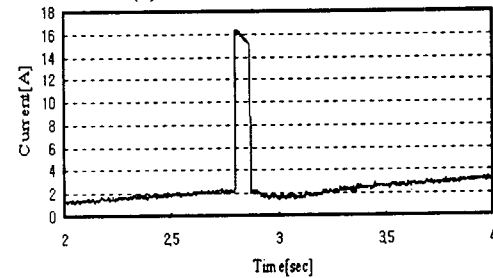
Fig. 8 Computer simulation results with optimal efficiency controller(1500rpm)



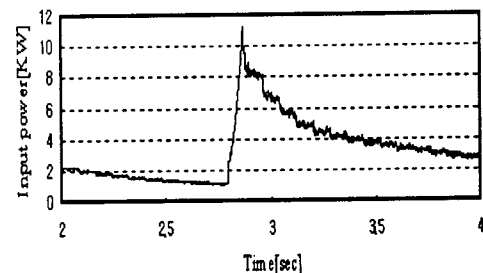
(a) rotor speed



(b) reference of flux current



(c) torque current



(d) input power

Fig. 9 Computer simulation results with optimal efficiency controller(450-900rpm)

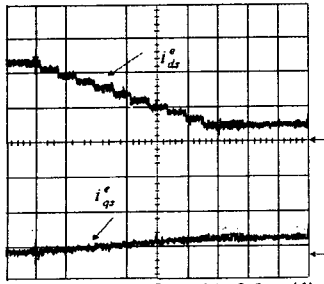


Fig. 10 Flux and torque current(500rpm, 0.1PU)

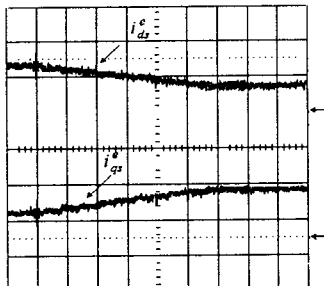


Fig. 11 Flux and torque current(500rpm, 0.5PU)

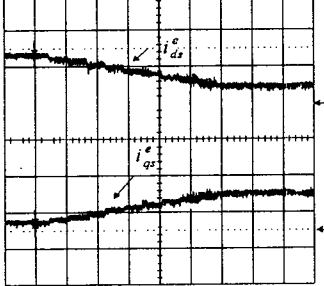


Fig. 12 Flux and torque current(1000rpm, 0.2PU)

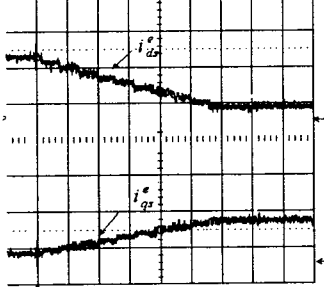


Fig. 13 Flux and torque current(1000rpm, 0.4PU)

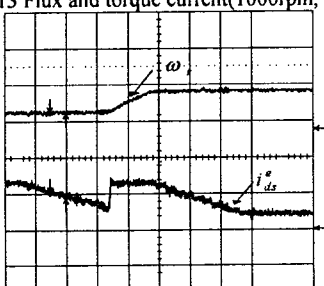


Fig. 14 Flux and torque current(500-1000rpm)

Experimental results show the performance of the proposed controller in Fig. 10-14. The characteristic waveforms in Fig. 10-14 are the flux and torque reference current at the speed of 500rpm, 1000rpm, and 500→

1000rpm. These waveforms are obtained by the proposed algorithm such as the computer simulations.

Experimental results show the performance of the proposed controller in Fig. 10-14. The characteristic waveforms in Fig. 10-14 are the flux and torque reference current at the speed of 500rpm, 1000rpm, and 500→1000rpm. These waveforms are obtained by the proposed algorithm such as the computer simulations. We can also see that all goes well. Figure 15 shows the efficiency characteristic curve. The figures show the capacities of the proposed control scheme when the speed reference and the load are varied. It has high efficiency for induction motor drives. The higher the speed is and the lower the load is, the higher the efficiency of the motor is.

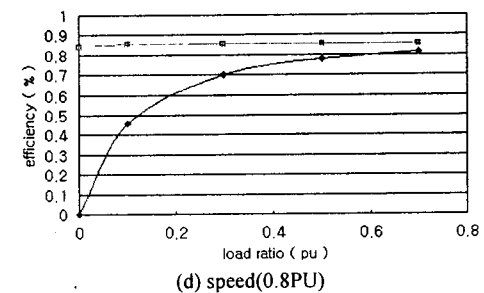
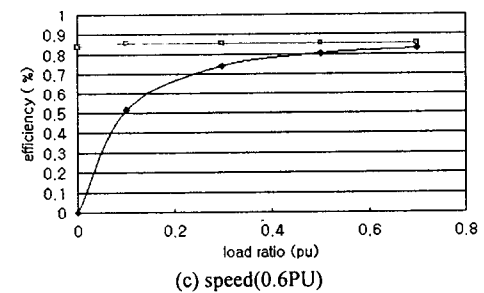
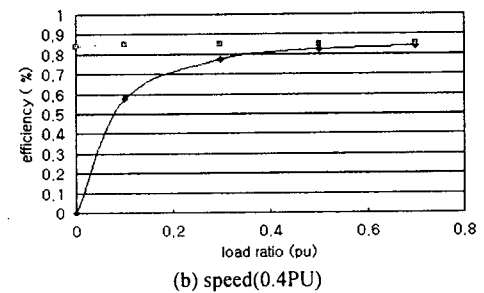
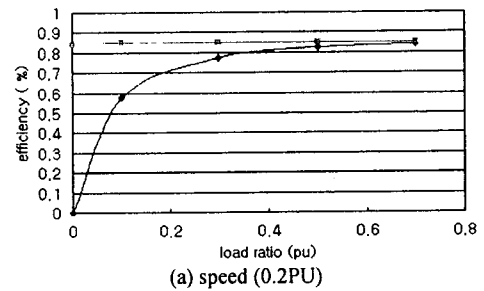


Fig. 15 Efficiency curve according to the speed and load
 (■ : Optimal flux, ▲ : Rated flux)

5. Conclusions

In this paper, the control algorithm for maximum efficiency drives of the induction motor system with the high dynamic performance is presented. We design the

simple model that includes equations of iron loss under the several assumptions. For the high efficiency, we may find out the optimal balanced point with this model. To reduce the input power of the induction motor, the flux and torque currents are controlled independently. The proposed controller is only operated in the steady state. According to the proposed optimal efficiency control algorithm, we come to know that the efficiency of the motor is higher at the higher speed and the lower load. Simulations and experiments, through the drive system with the proposed efficiency optimization controller, show the good performance for the vector control of the induction motor.

Reference

- [1] Dal Y. Ohm, Yuri Khersonsky and James R. Kimzey, "Rotor Time Constant Adaptation Method For Induction Motors Using DC Link Power Measurement", IEEE Trans. Ind App., pp588 - 593, 1989
- [2] P.Famouri and J.J cathy, " Loss minimization control of an induction motor drive." IEEE Trans. Ind App. Vol. 27.No.1,pp.33-37.Jan/Feb.1991
- [3] G.O.Garcia, J.C.Mendes Luis, R. M. Stephan, and E. H. Watanabe, " An Efficient Controller for an Adjustable Speed Induction Motor Drive", IEEE Trans. Ind. Elec., VOL. 41, NO.5, pp533 - 539, OCTOBER 1994
- [4] Gilberto C. D. Sousa, member, IEEE, Bimal K. Bose, and John G.Cleland, "Fuzzy Logic Based On-Line Efficiency Optimization Control of an Indirect Vector-Controlled Induction Motor Drive", IEEE, Trans. Ind. Elec., VOL.42,NO2 pp192 - 198, APRIL 1995
- [5] B.K.Bose, Powe Electronics and AC drives, Englewood cliff, NJ: Prentice hall.1986
- [6] Duck-yong Yoon,Gyu-Ha choe, Soon-chan Hong, Woo-Hyun Back, Eun-woong Lee."Maximum Efficiency Drive of Vector-controlled Induction Motors." KIEE. Vol.1.pp 27-37. Nov.1996

APPENDIX

Experiments have been realized using the following actual parameters of an induction motor :

2KW, 220/320V, 4.8/8.3A, 4poles, 1720rpm

$$\begin{array}{ll}
 R_r = 0.52 [\Omega] & R_s = 1 [\Omega] \\
 L_r = 103 [mH] & L_s = 110[mH] \\
 M = 103 [mH] &
 \end{array}$$